

MISALIGNMENT EFFECT FUNCTION MEASUREMENT FOR OBLIQUE ROTATION AXES: COUNTERINTUITIVE PREDICTIONS AND THEORETICAL EXTENSIONS

Stephen R. Ellis*, Bernard D. Adelstein*, Kiwon Yeom**
NASA*, San Jose State University Foundation**
NASA Ames Research Center, Moffett Field CA 94035

The Misalignment Effect Function (MEF) describes the decrement in manual performance associated with a rotation between a person's visual display frame of reference and that of their manual control. It now has been empirically determined for rotation axes oblique to canonical body axes and compared with the MEF previously measured for rotations about canonical axes. A targeting rule based on these earlier measurements is derived from a hypothetical process and shown to describe some of the data from three previous experiments. We call it the *Secant Rule*. It appears to explain the motion trajectories determined for rotations less than 65° purely in kinematic terms without a need to appeal to a process of mental rotation. Further analysis of this rule in three dimensions applied to oblique rotation axes leads to a somewhat surprising expectation that the difficulty posed by rotational misalignment should get harder as the required movement is shorter. This prediction is confirmed. Geometry underlying this rule also suggests analytic extensions for predicting more generally the difficulty of making movements in arbitrary directions subject to arbitrary misalignments.

INTRODUCTION

Though instrumentation, training or procedures can be used to manage the control difficulties posed by awkwardly oriented teleoperation cameras, users of remote systems need to be able to operate through rotated views of remote worksites to monitor automation. They also need to be prepared to take over in the case of failures. Indeed, in many cases the required instrumentation, sensors, and telecommunication may simply not be present to enable the partial automation needed to provide users with intuitive geometric relations between their control inputs and their end effector movements¹ Consequently, there is a need to understand the scientific basis of the control difficulties encountered when a telerobot user is faced with a rotation between the control frame of their input devices and their remote view of the worksite. This rotation constitutes a misalignment of two 3D frames of reference. The function relating the amount of misalignment to the decrease in user performance may be termed a Misalignment Effect Function (MEF)².

We define the Misalignment Effect Function as the relative decrement in the efficiency of user interaction with objects under user spatial control due to a rotation between their viewing or display coordinates and their control co-ordinates. There are a variety of ways this decrement may be measured, but we have chosen to use normalized Path Length (nPL) as our basic measure for theoretical reasons apparent below. Normalized Path Length is defined for any movement from a starting point to a target point as the path length actually moved divided by the minimum (straight-line) distance from the start point to the target (Ellis, Yeom, & Adelstein, 2012). Because nPL can be objectively related to optimal performance for purely translational movements, this definition also provides a path for extension to other aspects of movement since for extension all that is needed is an alternative optimality criteria. The movement in question then may sim-

ply be expressed as a proportion of the corresponding optimal movement.

In work reported last year (Ellis, et al, 2012)) we have used nPL to measure the empirical MEF for rotations that were either pure pitch, roll or yaws in an aeronautical coordinate system with +x forward away from the body. We showed that when results were integrated across all possible movement directions into the eight surrounding octants (see Figure 7), pure roll rotations about the x-axis showed a distinctly more difficult pattern than pure pitch or yaw rotations about +y +z respectively. We argued that this difference was due to the unique steering roles of both lateral and vertical control. Roll rotations disturb control in both of these axes but pitches or yaws only affect one of the two.

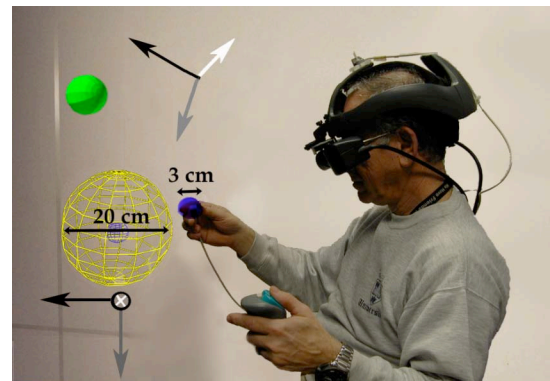


Figure 1. This composited exocentric view shows a participant in our immersing virtual environment moving a computer-generated blue cursor ball to touch the larger, flat-shaded green, spherical target at the upper left. Participants used a physical hand-held control to initiate trajectory recording and advancement to the next target (See Ellis *et al*, 2012 for details). The wire-frame sphere encircling the start point, shown for scale, disappeared on trial start. The two coordinate frames, not visible during testing, show a multi-axis rotational misalignment between the display axes (lower left) and the control axes (upper left-center).

We were also able to show that the first $\sim 1/3$ of the MEF revealed a gradual loss of efficiency so that ultimately about twice as much path length is produced as rotations approach $\sim 65^\circ$ (Fig. 2). We

¹ See Macedo, Kaber, Endsley, Powanusorn, & Myung, 1998, or design descriptions of the Intuitive Surgical *Da Vinci* telerobot for example of such partial automation.

² Formerly called the Misalignment Disturbance Function (MDF)

proposed through a purely geometric argument that a simple targeting rule can explain this part of the MEF.

In the following paper we first review our previous results and derive our targeting rule in more detail (Fig. 3). We then extend our measurement of the MEF in the experiment described below to rotations that may be more representative of those actually encountered in the field in that they are not about canonical axes. In fact, the rotations that we have selected for the present experiment may seem more complicated than rotations about canonical axes because their descriptions in terms of euler angles or quaternions are not easily verbalized. We will show that such descriptive approaches focusing only on the rotations may actually miss the central feature which makes control in a rotated frame difficult .

Fig. 1 illustrates the basic movement task that we have used. Participants were placed in a simple virtual environment. They were instructed to move their hand to a central point in a large wire-frame sphere. Next, following the participant’s button press, a target would randomly appear some distance from the starting point. They were thereafter to control a cursor by moving their spatially tracked hand so as to make the cursor touch the target, after which the target then vanished. Participants would then return their hand to the center to prepare for the next target.

As in our previous work, our focus is on users’ ability to overcome disturbances due to the unusual visual motion of the controlled element caused by experimentally imposed rotational misalignment. We believe the underlying control difficulty under input-display frame misalignment originates in the disturbance of the motion feedback that would otherwise help steer the users motion. Consequently, to exclude rotational cueing information from visually or kinesthetically sensed structures in our experimental studies, we restrict ourselves to spherical display elements. Ultimately, we seek to develop a general theory that will enable us to predict the underlying control difficulty for user movement toward an arbitrary target location subject to an arbitrary rotational misalignment.

A Partial Theory of the MEF

Fig. 2 summarizes some results from last years HFES Proceeding report in which the MEF was determined by pooling rotations about the canonical pitch, yaw and roll axes. The resulting function is usefully discussed in terms of three parts: the first slowly increasing part up to about 65° of rotation, the second more rapidly increasing part leading to a peak around 120° of rotation, and a third with a distinctive decrease coming down to a level at 180° well above that of 0° degree rotation. All of these features must be explained by a complete theory of the MEF. We will focus only on the first part below 65° but will also comment in the Discussion section on rotations at and above 90°.

It is tempting to explain the MEF in terms of internal user information processing which might involve mental rotation. Such processing may well be involved, especially with respect to the larger rotations. However, since the disturbance of user performance is inherently geometrical, it is informative to first look towards geometrical explanations that involve simple, possible targeting rules.

In particular, we have examined a targeting rule that essentially is a definition of visual-motor coordination and assumes that human movements are made up of submovements as posited by the sample-data control introduced long ago in movement models (Stark, Iida & Willis, 1961, (See Fig. 3) The rule is: First, set current kinesthetic direction, \mathbf{x}_{i+1} equal to visual direction at submovement start i.e., \mathbf{x}_i . Second, iterate across all submovements starting with \mathbf{x}_0 until contact is made with the target. Implicit in this rule is that completed human hand movement paths are inherently made of a pattern of progressively refined submovements arising from the sample-data control at the heart of vertebrate kinesiology (e.g. Stark, Iida & Willis, 1961, Crossman & Goodeve, 1983)

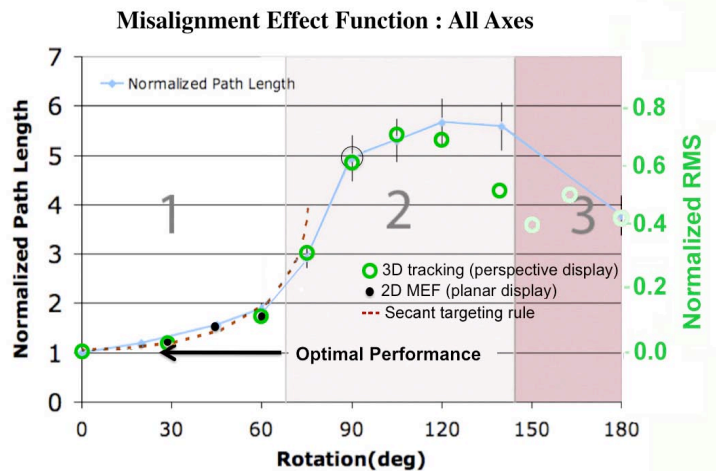


Figure 2. The MEF resulting from pooling results from Ellis, Yeom, & Adelstein (2012) for rotations about pitch, roll, and yaw for a task like that in this paper. For comparison, results from a related 2D placement task published previously are overlaid (Ellis & Adelstein, 2009). Also overlaid are results from a 3D tracking task done on a perspective display with display-control coordinate misalignments (Ellis, Tyler, Kim & Stark, 1992). These datasets show MEF similarity for the three response measures³

As shown in Fig. 3, integration across all of a movement’s constituent submovements yields a simple expression for the expected nPL. Since $1/\cos(\psi) = \sec(\psi)$, we call this expression the *Secant Rule* for coordinated hand movement. In fact, this targeting defines an equivalence class over velocity profiles since a wide variety of profiles will give rise to trajectories of the same general form, though the piece-wise approximation to the equiangular spiral will vary. This equivalence class over a variety of velocity profiles is directly analogous to the equivalence class over ratios of movement distances to target widths defined by Fitts’ Law⁴. One can see in Fig. 2 that the targeting process provides a fairly good fit to the empirical MEF for rotations less than ~65°, and it’s without free parameters! Clearly, this simple targeting must breakdown at some point since as $\psi \rightarrow 90$, $\sec(\psi) \rightarrow \infty$ where the targeting rule produces an orbit around the target. The targeting process must change at or near this point.

³ Data from other laboratories also could be plotted onto this figure if their dependent measure can be normalized to an optimal behavior.

⁴ Deeper connections to Fitts’ Law exist which show that target width plays the role of a normalizing factor but they are out of this paper’s scope.

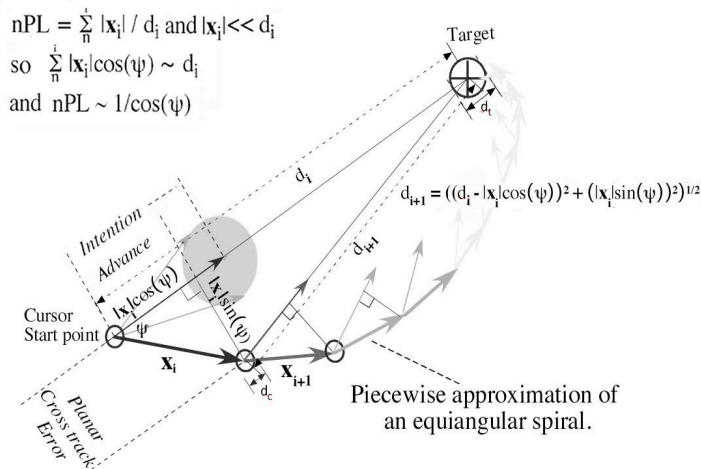


Figure 3. Iterative targeting rule geometry where $intention_i = x_i$ and the derivation of the *Secant Rule* is sketched.

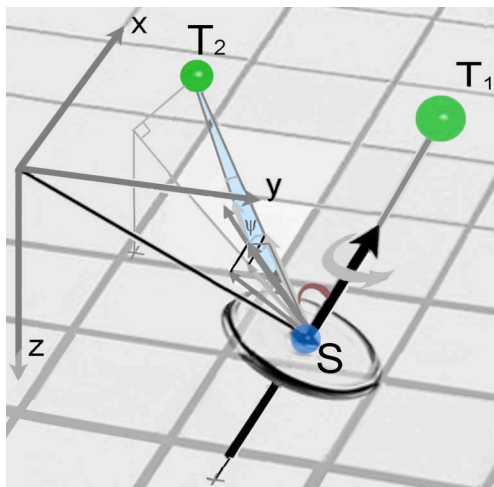


Figure 4. Targeting rule visualized more generally in 3D space showing a part of the plane of action (light blue) determined by intended direction of movement (lightest vectors) and the achieved direction of movement (darker vectors).

The range of conditions over which of the proposed targeting rule applies is probably determined by an optimization process analogous to that suggested for raptors which also move, i.e. fly, along equiangular spirals when they dive onto their prey. They do so because from their normal surveillance height they must target their prey with their high resolution fovea which is rotated laterally $\sim 45^\circ$ with respect to their body axis (Tucker, 2000). It appears the birds fly time-optimally by trading off the longer flight path needed to maintain use of their hi-res fovea against the added speed they can achieve by avoiding head turning that slows them down. Human telerobot operators may similarly trade off the time to move along an equiangular spiral against the added time and effort needed to determine a compensatory path. This trade off may be reasonably expected since arm control models are frequently time optimal. The operative ratio that influences the human user's trade off would seem to be the *advance / intention* ratio as indicated in Figs. 3 and 4. This ratio is, in fact given by $\cos(\Psi)$, where Ψ is the rotation angle. Data to date suggest the critical value for this ratio is around 0.56, which corresponds to

$\cos(65^\circ)$, where 65° is approximately the largest rotation for which the *Secant Rule* applies. The critical value could be interpreted as the minimum acceptable efficiency factor with which the *advance* brings the operators controlled element towards their targets (Fig. 3, 4 and 5). Interestingly, this factor is reminiscent of the constant, A , used by Crossman and Goodeve (1983) in their derivation of Fitts' Law, representing the proportion of the remaining distance moved to the target after each submovement. This parallel suggests development of a Fitts Law for off-axis movement.

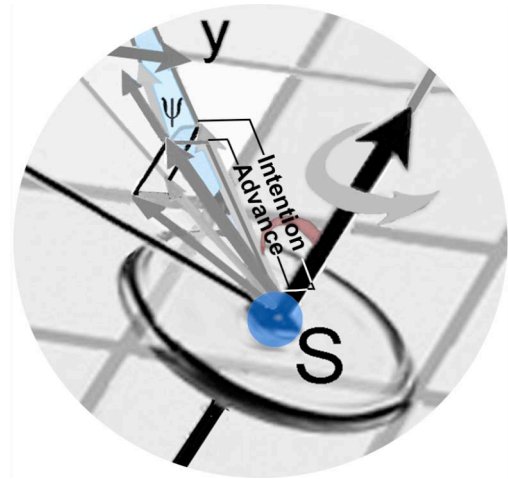


Figure 5. Enlargement of targeting rule visualization in 3-D space. The rotation Ψ of the intended movement vector (lightest arrow) to the achieved movement vector (dark arrow) defines the light blue *plane of action*.

Curiosity regarding generalization of the MEF to rotations about noncanonical axes naturally arises and we have begun to investigate more generalized conditions in the following experiment. In order to think about the possible effects of such rotations on the MEF we have extended the geometry of Fig. 3 to 3 dimensions in Fig. 4. This figure represents an arbitrary rotation associated with an arbitrary motion from start point S to target T_2 . The rotation axis is represented by the thick dark black arrow passing through S . The arc around the axis shows the amount of rotation. The plane of rotation is represented by a disk centered at S . Any possible rotation may be represented as done in Fig. 4.

For rotations that we previously used about the canonical axes, all planes of rotation were *ipso facto* parallel to the canonical surfaces orthogonal to the rotation, e.g. roll rotation about the x -axis has a plane of rotation parallel to the y - z plane. These rotation conditions are relatively easily described and understood by participants. But they are very special cases. A full theory of the MEF must extend beyond them as shown in Fig. 4.

Consideration of Figure 4 as representing an arbitrary rotation leads to some qualitative conclusions from the geometry which we investigate in the experiment below, deferring a more quantitative analysis for future reports. For example, one can immediately see that the specific position of the target with respect to the rotation axis can have a major influence on the effect of the rotation: Targets positioned exactly on the axis, e.g. T_1 are unaffected by the rotation. Those in the plane of rotation itself are maximally affected. This fact, however, is very much influenced by user-produced translational and directional noise that we do not con-

sider it at length for this paper. Another interesting inference; however, is that accurate targeting will result in a path in a planar spiral within what we call the *plane of action*. This plane is determined by the direction of the target, e.g. T_2 with respect to the starting point, the starting point S , and the orientation of the plane of rotation. One can see that this is indeed a plane by noting that the grey vector representing an initial intended submovement towards the target and the darker vector representing the actual movement after the rotation define a plane containing the target. Subsequent accurately intended submovements are also in the same plane because they originate in the plane, are directed to the same point and are rotated in a parallel plane.

It is interesting to note that there is a great advantage for participants who can stay in the initial *plane of action* shown in Figs. 4 and 5. Staying in this plane turns their targeting task into a simpler one-degree-of-freedom (dof) problem instead of a two-dof problem. Accordingly, because displacement noise that takes the cursor out the *plane of action* has a much greater effect on the directional corrections needed to return to the plane as the cursor approaches the target, one might expect targeting to become more difficult for nearer targets than for farther ones. This effect is enhanced by the slowing of cursor motion as one gets closer to the target, which, in turn, makes visual discrimination of the error more difficult. We investigate this possible effect of distance in this experiment.

METHODS

Subjects: Ten unpaid volunteers aged 24-65 participated. Eight were men; two were women. Subjects were screened for stereo vision, compatibility with the head-mounted display and provided IRB required consent for human experimentation,

Head mounted display: A modified Rockwell-Collins SR80 binocular head mounted displays was used. Descriptive details may be found in our previous paper and manufacturer specifications (Ellis, et al, 2012).

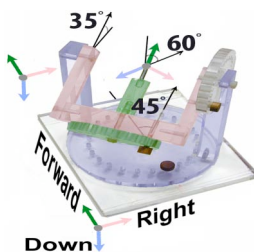


Figure 6. Helmholtz gimbal illustrating yaw-pitch-roll euler component rotations for one of the rotations used in the experiment.

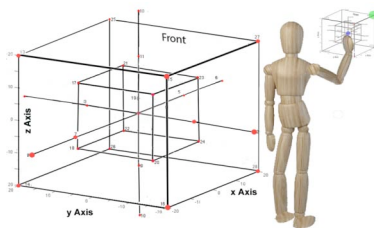


Figure 7. shows the approximate positions of the 28 targets used for the two target distances.. Movements were from the center outward targets. Separate randomized sequences of targets were used for blocks of targets subject to a fixed rotation for each participant.

Computer hardware and software: The experiment was run in a custom-written Virtual Environment (VE) authored by Richard H. Jacoby, using lower-level tracking sensor interface software by AuSim, Inc. The programs ran under Windows XP (SP2), sampling tracker positions at 120 Hz, rendering at 60 fps, with a measured full system latency of ~ 30 ms. See (Ellis, et al., 2012).

Experimental virtual environment: The VE created for the study was a simple room with dimensions roughly matching the physical room (4.0 x 4.5 x 2.9 m) in which the experiment was conducted. Diffuse lighting coming from virtual room sources mimicked the lighting in the real room. Texture maps that corresponded approximately to the room's actual ceiling and floor provided some additional realism.

Experimental design: A more detailed description of our general experimental procedure may be found in our previous paper (Ellis, Yeom, & Adelstein, 2012). It is important to reiterate here that the subjects were told that when their task got harder, the goal of their movement was to try to move as they did when the task was easy during initial familiarization. We put no specific premium on quick motion onset, speed, or accuracy.

Independent variables. 1) Target distance from the origin centered in front of the participant, at two levels: 11 cm or 22 cm. 2) Control-to-display coordinate rotation in terms of yaw, pitch, and roll angle⁵ respectively: $(\pm 45^\circ, 35^\circ, 0^\circ)$, $(\pm 45^\circ, 35^\circ, \pm 30^\circ)$, $(\pm 45^\circ, 35^\circ, \pm 60^\circ)$, $(\pm 45^\circ, 35^\circ, \pm 90^\circ)$. Note that the signs for yaw and roll angles were matched for each Euler triple, yielding eight rotation levels. This sign matching resulted in symmetrical poses of the final Euler rotation axis⁶, e.g., $(+45^\circ, 35^\circ, +30^\circ)$ is symmetric with the triple $(-45^\circ, +35^\circ, -30^\circ)$. Ultimately, we collapsed rotation across signs, as we found no reliable asymmetries in the performance data..

Dependent variables: Normalized Path length (nPL) was used as our principal measure for analysis. This measure is a kind of efficiency measure, essentially a kind of per cent calculation that we infer also reflects task difficulty on the presumption that subjects are consistently striving for the same efficiency when they “try to move as they did when the task was easy.”

RESULTS

Fig. 8 plots the two significant main effects confirming the somewhat counterintuitive prediction that, at least in terms of normalized Path Length, movement towards the near targets is relatively longer and less efficient. There was no statistical interaction as is evident from the parallel traces of the two presented distance conditions. Note that the final 90° rotation has a much smaller effect than a single 90° about a canonical axis (Fig. 2).

DISCUSSION

Because the present somewhat counterintuitive results are based on presumptive constant noise or jitter present in human motion, they emphasize that any full theory of the control difficulty introduced by a display control rotation needs not only to predict the biases in errors but also the variances that are introduced. In this context we have observed in our data that variances in normalized Path Length for the first part of the

⁵We use a standard aeronautical coordinate system with yaw carrying pitch carrying roll illustrated in Fig. 6.

⁶We refer to symmetry of the Euler axes not the final gimbal element.

MEF are a linear function of the introduced rotation. We plan to include this aspect of our data in future more complete targeting models as we lack adequate space in the present report

A second observation that we can make is based on a comparison of performance under pure pitch, yaw, or roll rotations of 60° and 90° from our prior study (Ellis et al., 2012) versus performance in the present experiment where roll (the third component of our Euler rotation sequence) of the same magnitude is instead applied following underlying yaw and pitch rotations. Despite the fact that the resulting poses in the present experiment are much more difficult to describe, our participants' behavior was much less affected by these compound Euler rotation sequences than pure pitches, yaws, or rolls. This difference is likely due to a difference in the average ratio of advance-to-intention movement components.⁷ This difference is striking in that the 90° rotation about any of the principle axes drives the *advance* to zero and renders totally inoperative the targeting rule we have described. However, something akin the *Secant Rule* still works for the rotations created by the compound Euler sequences as we can attest from personal experience in the experiment for conditions in which the last rotation in the sequence, roll, was set to 90°.

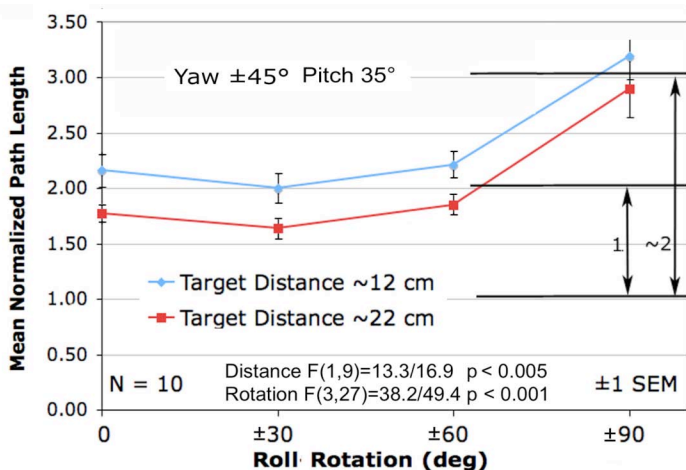


Figure 8. Results for ANOVA F's for raw/skew-corrected log transformed data shown respectively. Performance ranged over about a factor of two with respect to optimal performance.

A final comment regarding our *Secant Rule* is noteworthy in that it provides an explanation for a phenomenon reported in by Abeele and Bock (2001). When testing transfer of sensorimotor adaptation to rotational misalignments, they noticed that participants who adapted to fixed rotations less than 90°, showed transfer to other rotations less than 90° but not to rotations greater than 90°. Conversely, those adapting to rotations greater than 90°, only showed transfer to other larger rotations. Our rule explains this pattern. Transfer from small to large rotations doesn't occur because no amount of training will make the *Secant Rule* work for large rotations. Clearly, a different rule must be used for large and small rotations.

In the end it may be necessary to appeal to "mental rotation" as an explanation for some aspects of the MEF, but we hope, those who take this approach, ourselves included, realize the violation of Occam's Razor that such a tack involves. Appealing to a concept itself not well understood hardly promises an explanation that could have the ring of truth. In any case there are specific difficulties in any appeal to mental rotation. Careful measurement of the MEF generally shows that as the rotation angle increases past 120° towards 180°, there is a clear drop in the function showing the task getting easier. This drop seems to be associated with motor performance. (Chintamani, et al, 2010). Classic mental rotation functions, in contrast usually associated with perception or discrimination, continue to increase consistent with the idea that a more or less constant, covert rate of rotation introduces a continuous increase in the participants' response times (Shepard & Metzler, 1971, but see Collishaw & Hole, 2002).

It must be noted, however, that the decrease of the MEF may not be seen in experiments without sufficient statistical power or appropriate experimental design to reduce the significant noise associated with function measurements at the large rotations. Indeed, any explanation of this later part of the function also needs to explain this increased noise. Our expectation in this respect is that the noise arises from ambiguities and uncertainties as to the orientation of the error vector when targeting errors of submovements are noticed. These ambiguities, which may essentially amount to errors in understanding the local principal surface normal, could result in large incorrect "corrective" movements out of the initial *plane of action* and could, by an argument parallel to the one we've made about the target approach, also explain the rise in trajectory variability for the large rotations.

Acknowledgment: NASA HRP Space Human Factors Engineering.

REFERENCES

- Abeele, S. & Bock, O. (2001) Sensorimotor adaptation to rotated visual input: different mechanisms for small vs large rotations. *Exp. Brain Res.*, 140, 407-410.
- Chintamani, K. K., Cao, A. Ellis, R.D. & Pandya, A.K. (2010) Improved telemanipulator navigation during display-control misalignment using augmented reality cues. *IEEE Trans. Sys. Man & Cyber.(A). Sys. & Humans*, 40, 1, 29-39
- Collishaw, S.M. & Hole, G. J.(2002) Is there a linear or nonlinear relationship between rotation and configural processing. *Perception*, 31, 287-296.
- Crossman, E.R.F.W. & Goodeve, P. J. (1983) Feedback control of hand-movements and Fitts' law. *Quarterly J. of Exp. Psych.*, 35A, 251-278.
- Ellis, S. R., Tyler, M., Kim, W. S., & Stark, L. (1992) Three-dimensional tracking with misalignment between display and control axes. *SAE Transactions.: J. of Aerospace*, 100-1, 985-989.
- Ellis, S.R. & Adelstein, B.D. (2009) Kinesthetic compensation for sensorimotor rearrangements. *J. of Motor Behav.*, 41, 6, 501- 518.
- Ellis, S.R., Yeom, K. & Adelstein, B.D. (2012) Human control in rotated frames: anisotropies in the misalignment disturbance function of pitch, roll, and yaw. Proc. HFES, October, pp. 1336-1341.
- Macedo, J.A., Kaber, D.B., Endsley, M.R., Powanusorn, P., & Myung, S. (1988) The effect of automated compensation for incongruent axes on teleoperator performance. *Human Factors*, 40, 4, 541-553.
- Stark, L, Iida & Willis, P.A. (1961) Dynamic characteristics of the motor coordination systems in man. *Biophysical Journal*, 1, 279-300.
- Shepard, R & Metzler, J. (1971) Mental rotation of three dimensional objects. *Science*, 171, 972, 701-3.
- Tucker, Vance A. (2000) The deep fovea, sideways vision, and spiral flight paths in raptors. *J. of Exp. Biology*, 203, 3745-3754.
- Yeom, K, Adelstein, B.D., & Ellis, S.R. (2012) Determining the discontinuities for three-dimensional trajectory data in teleoperation. Proc HFES, October 2012. pp. 2537-25411.

⁷ We will calculate this ratio for the final paper; it is not ready for the proposal due to the need to evaluate nonlinearities in directional data..